Tributaries and Deltas: Efficient and Robust Aggregation in Sensor Network Streams

Amit Manjhi
Carnegie Mellon Univerity
manjhi@cs.cmu.edu

Suman Nath
Carnegie Mellon University
sknath@cs.cmu.edu

Phillip B. Gibbons
Intel Research Pittsburgh
phillip.b.gibbons@intel.com

ABSTRACT

Existing energy-efficient approaches to in-network aggregation in sensor networks can be classified into two categories, tree-based and multipath-based, with each having unique strengths and weaknesses. In this paper, we introduce Tributary-Delta, a novel approach that combines the advantages of both the existing approaches by running them simultaneously in different parts of the network. We study this new approach, present schemes for adjusting the balance between different components of the aggregation topology in response to changes in network conditions, and show that many useful aggregates can be readily computed within this new framework. We then show how a difficult aggregate for this context—finding frequent items—can be efficiently computed within the Tributary-Delta framework. To this end, we devise the first algorithm for frequent items (and for quantiles) that provably minimizes the worst case total communication for non-regular trees. In addition, we give a multi-path algorithm for frequent items that is considerably more accurate than previous approaches. Through extensive simulation with real-world and synthetic data, we show the significant advantages of our techniques. For example, in computing Count under realistic loss rates, our techniques can reduce errors by up to a factor of 3 compared to *any* existing techniques.

1. INTRODUCTION

Networked collections of smart sensors are increasingly being used to monitor and query the physical world. These small sensor *motes* are typically battery-powered, possess limited CPUs and memory, and organize themselves into ad hoc multi-hop wireless networks around more capable base stations. A paramount concern in these sensor networks is to conserve the limited battery power, as it is usually impractical to install new batteries in a deployed sensor network. Because the battery drain for sending a message between two neighboring sensors exceeds by several orders of magnitude the drain for local operations within a sensor mote, minimizing sensor communication is a primary means for conserving battery power [1, 20]. Thus for aggregation queries (e.g., the average temperature reading across the sensor network), it is now accepted practice [11, 12, 24, 25] that aggregates are computed *in-network* whenever possible—this avoids the excessive communication required to route all the sensor readings to the base station. With the in-network approach, sensor readings are accumulated into partial results that are combined as messages propagate toward the base station. In many common cases (such as Sum, Count, Average, Min, Max), each sensor node transmits only one short message during the aggregation—a considerable energy savings over the route-all approach.

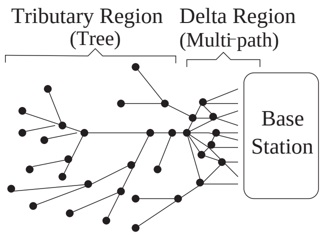

Figure 1: Tributaries and Deltas

Existing energy-efficient approaches to in-network aggregation can be classified into two categories: tree-based and multi-path-based. In the tree-based approach (such as in TAG [11], TinyDB [12], and Cougar [24]), a spanning tree, rooted at the base station, is constructed for use in answering queries. Subsequently, each query answer is generated by performing in-network aggregation along the tree, proceeding level-by-level from its leaves to its root. Many aggregates (including those given above) can be computed exactly and with minimal communication on a tree topology, assuming no communication failures. However, wireless sensor networks have high communication failure rates (up to 30% loss rate is common [11]), and each dropped message results in an entire subtree of readings being dropped from the aggregate answer. As a result, it is not uncommon to lose 85% of the readings in a multi-hop sensor network, causing significant answer inaccuracy [17].

To overcome the severe robustness problems of the tree approach, Considine *et al.* [5] and Nath *et al.* [17] recently proposed using multi-path routing for in-network aggregation. Instead of having each node send its accumulated partial result to its *single* parent in an aggregation tree, the multi-path approach exploits the wireless broadcast medium by having each node broadcast its partial result to *multiple* neighbors. Both papers recommend a topology called *rings*,

	Energy Components			**Error Components**			**Latency**
	Number of messages	**Message size**		**Communication error**	**Approximation error**		
Aggregate:	*any*	*Count*	*Freq.Items*	*any*	*Count*	*Freq.Items*	*any*
Tree [11, 12, 24, 25]	minimal	small	medium	very large	none	small	minimal
Multi-path (rings) [5, 17]	minimal	small	large	very small	small	small	minimal
Tributary-Delta [this paper]	minimal	small	medium	very small	very small	small	minimal

Table 1: Comparison of previous in-network aggregation approaches and the Tributary-Delta approach. The total energy consumption is given by its two components. The total error is given by the sum of the *communication error* produced by message losses within the network and the *approximation error* coming from the aggregation algorithm (independent of message loss). Because the message size and approximation error depend on the aggregate, these metrics are shown for two representative aggregates: Count and Frequent Items.

in which the nodes are divided into levels according to their hop count from the base station, and the multi-path aggregation is performed level-by-level toward the base station. This approach sends the same minimal number of messages as the tree approach (i.e., one transmission per node), making it energy-efficient. It is also very robust to communication failures because each reading is accounted for in many paths to the base station, and *all* would have to fail for the reading to be lost. However, there are two drawbacks to the multi-path approach: (1) for many aggregates (e.g., Count, Sum, Average) the known energy-efficient techniques provide only an *approximate* answer (with accuracy guarantees), and (2) for some aggregates, the message size is longer than when using the tree approach, thereby consuming more energy.

The first two rows of Table 1 provide a qualitative comparison of the previous in-network aggregation approaches. As the table shows, the tree approach suffers from very high communication error while the multi-path approach can have larger message sizes and approximation errors.

Tributary-Delta. In this paper we present a new approach to in-network aggregation that combines the advantages of both the tree and multi-path approaches, by dynamically adapting the aggregation scheme to the current message loss rate. Under low loss rates, trees are used for their low or zero approximation error and their short message size. Under higher loss rates or when transmitting partial results accumulated from many sensor readings, multi-path is used for its robustness. We call our approach *Tributary-Delta* because of the visual analogy to a river flowing to a gulf: when far from the gulf, the merging of river *tributaries* forms a tree-like shape, whereas near the gulf, the river branches out into a multi-path *delta* in order to reach the gulf despite the increased obstacles (see Figure 1).

We show that our Tributary-Delta approach significantly outperforms both previous approaches. An example result is shown in Figure 2 (full details in Section 7). As expected, the tree approach is more accurate than the multi-path approach at very low loss rates, because of its lower approximation error (0% versus 12%). However, at loss rates 0.1 or higher, tree is much worse than multi-path because of its high communication error. On the other hand, Tributary-Delta is able to provide not just the best of both (e.g., by running either tree or multipath in the whole network), but in fact a significant accuracy improvement over the best, across a wide range of loss rates—thus demonstrating the synergies of using both in tandem. The last row of Table 1 summarizes the benefits of Tributary-Delta.

To enable simultaneous use of the tree and multi-path

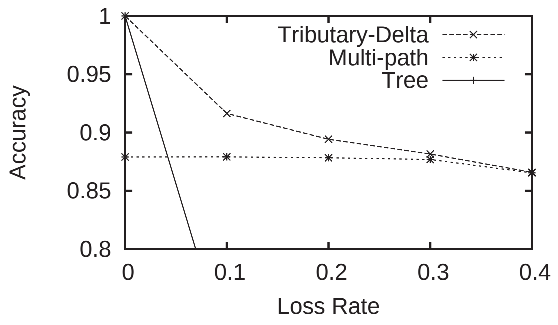

Figure 2: Accuracy of a Count query under varying message loss rates. The experimental setup and the full graph are provided in Section 7.

aggregation approaches, we must resolve several challenges. For example, how do the nodes decide whether to use the tree or the multi-path aggregation approach? How do the nodes using different approaches communicate with each other? How do the nodes convert partial results when transitioning between approaches? We identify and address these and other challenges and issues in this paper, through a careful system design and algorithmic study. We also discuss how a large number of aggregates can be computed within the Tributary-Delta framework.

Our most significant algorithmic result is a new Tributary-Delta algorithm for finding frequent items. For this result, we devise a new tree-based algorithm, a new multi-path-based algorithm, and a new (combined) Tributary-Delta algorithm. Previous *tree-based* frequent items algorithms worked only for balanced, regular trees [14] and/or used too much communication [8, 14]. We present the first frequent items algorithm that provably minimizes the worst case total communication for non-regular trees with certain properties common to typical sensor network deployments. In addition, our new *multi-path* algorithm uses low total communication while providing high accuracy; the only previous approach [17], based on sampling, is far less accurate.

In summary, the main contributions of this paper are:

- We introduce the Tributary-Delta approach to in-network aggregation in sensor networks, for adapting the aggregation scheme to current message loss rates. We show that many aggregates can be readily computed in this framework.

- We present schemes for adjusting the balance between tributaries and deltas in response to changes in network conditions.

- We show how a difficult aggregate for this context—finding frequent items—can be efficiently computed in the framework. To this end, we devise the first algorithm for frequent items (and for quantiles) that provably minimizes worst case total communication for non-regular trees. The algorithm's guarantees hold for a class of trees that arise naturally in sensor networks; we also present a new tree construction algorithm well-suited to generating trees in this class. In addition, we give a multi-path algorithm for frequent items that is considerably more accurate than the previous approach.

- We provide an extensive evaluation of Tributary-Delta aggregation on a realistic sensor network simulator, using real world and synthetic data sets, confirming the significant advantages of our techniques. For example, in computing Count under a typical loss rate ($0-40\%$), Tributary-Delta can reduce errors by up to a factor of 3 compared to an oracle that can dynamically choose the best existing approach (tree-based or multi-path-based) for a given loss rate. Moreover, Tributary-Delta never performs worse than such an oracle.

Although the general framework encompasses optimizing many possible metrics based on the criteria in Table 1, in this paper we focus on the following setting. Users provide target thresholds on both the communication error (e.g., at least 90% of the nodes should be accounted for in the answer) and the approximation error (e.g., the answer should be within 10% of the actual answer on those nodes). Our goal is to achieve these thresholds while incurring minimal latency, minimal number of messages, and minimizing the message size.

Roadmap. Section 2 describes background information and related work. Section 3 overviews our Tributary-Delta approach. Section 4 presents our adaptation design. Section 5 discusses Tributary-Delta algorithms for many aggregates. Section 6 presents our frequent items algorithm. Section 7 presents our experimental results. Finally, Section 8 presents conclusions.

2. PRELIMINARIES AND RELATED WORK

There has been a flurry of recent papers on energy-efficient, in-network computation of aggregate queries in sensor networks [5, 6, 8, 11, 12, 13, 17, 19, 21, 24, 25]. As discussed in Section 1, this previous work can be classified according to the aggregation topology used: tree-based or multi-path-based. In this section, we describe these two approaches in more detail and survey the related work. We begin by describing the general set-up used in this paper.

Aggregation Set-up. We have m sensor nodes each generating a stream of sensor readings. The sensor nodes are connected (either directly or via other sensor nodes) to a base station. Aggregate queries, which may be one-time or continuous, are sent from the base station to all the nodes. Queries may aggregate over a single value at each sensor (e.g., the most recent reading) or over a window of values from each sensor's stream of readings. Each sensor node evaluates the query locally (including any predicates), and produces a local result. There is an aggregation topology (e.g., tree or rings) that is used to route these local results to the base station, combining them along the way into concise partial results. For continuous queries, the process of computing, routing and combining local results repeats itself at regular intervals, possibly in a pipelined fashion within the network [11].

We consider the realistic setting where the communication between sensors maybe lossy, and network conditions change over time. In evaluating the quality of an answer, we consider both the *communication error*, which results from message losses in the network, and the *approximation error*, which results from lossy data reduction performed to reduce message lengths [17].

Tree-Based. In the tree-based approach [6, 8, 11, 12, 13, 19, 21, 24, 25], a spanning tree rooted at the base station is constructed for use in answering queries. Each node computes its *level* (i.e., hops from the root) in the tree during this construction by adding one to the level of its parent. In-network aggregation proceeds level-by-level toward the root, starting with the nodes at the highest level. To coordinate the sending and receiving of messages, nodes are loosely time synchronized and are allotted specific time intervals (according to their level) when they should be awake to send and receive messages. In this way, level i nodes are listening when level $i+1$ nodes are sending. The period of time allotted for exchanging messages between two levels is called an *epoch* [11]. Epochs must be sufficiently long such that each sensor in a level can transmit its message once without interference from other sensors' transmissions. The *latency* of a query result is dominated by the product of the epoch duration and the number of levels.

To adapt the tree to changing network conditions, each node monitors the link quality to and from its neighbors [25]. This is done less frequently than aggregation, in order to conserve energy. If the relative link qualities warrant it, a node will switch to a new parent with better link quality, in order to make the tree more robust [25]. However, because each lost message drops an entire subtree, even trees with high link quality produce very inaccurate answers once the tree is beyond a certain size. This inaccuracy can be seen in Figure 2.

A key advantage of using a tree topology is that aggregating within the network is often straightforward, using minimal resources and incurring no approximation error. For example, for a Sum query, each node transmits the sum of the readings in its subtree, by listening for its children's subtree sums, adding them to its own readings, and sending the result to its parent. In the absence of communication error, the resulting sum would be exact.

Multi-Path-Based. The multi-path-based approach [5, 17] allows for arbitrary aggregation topologies, beyond a tree. In this paper, we focus on the *rings* topology, because it provides a good energy-robustness trade-off [5, 17]. To construct a rings topology, first the base station transmits and any node hearing the transmission is in ring 1. At each subsequent step, nodes in ring i transmit and any node hearing the transmission—but not already in a ring—is in ring $i+1$. The ring number defines the level of a node, and the aggregation proceeds level-by-level, with level $i+1$ nodes transmitting while level i nodes are listening. In contrast to trees, the rings topology exploits the wireless broadcast medium by having *all* level i nodes that hear a level $i+1$ partial result incorporate that result into their own. This significantly increases robustness because each reading is accounted for in many paths to the base station, and *all* would have to fail for the reading to be unaccounted for in the query result. As with trees, nodes can monitor link quality and change levels as warranted.

A key advantage of using a rings topology is that the communication error is typically very low, in stark contrast with trees. This can be seen in Figure 2, where the accuracy of multi-path decreases very slowly with increasing loss rates (the approximation error is around 12% in this experiment, independent of the loss rate). Moreover, the rings approach uses the same minimal number of messages as the tree approach (i.e., one per node), making it energy-efficient.

However, because each partial result is accounted for in multiple other partial results, special techniques are required to avoid double-counting. Previous work has shown how to avoid double-counting in computing Count, Sum [5] and many other aggregates [17]. For this paper, we adopt the terminology of [17], where the multi-path approach is called *synopsis diffusion*.[1] There are three functions used to compute an aggregate: (1) A *synopsis generation (SG)* function that takes a stream of local sensor readings at a node and produces a partial result, called a *synopsis*; this function is applied by each sensor on its local readings. (2) A *synopsis fusion (SF)* function that takes two synopses and generates a new synopsis that summarizes both; this function is applied when combining partial results in-network. (3) A *synopsis evaluation (SE)* function that translates a synopsis into a query answer; this function is applied at the base station. We next illustrate these functions using the Count aggregate; this example highlights one of the clever techniques used to avoid double-counting in the multi-path approach.

Example 1. Consider answering a Count query requesting the number of live sensors. To avoid double-counting, we view the `Count` query as a `Count Distinct sensor-id` query, and use a well-known distributed distinct-values counting algorithm [7], as follows [5, 17]. Let n be a (possibly loose) upper bound on the total number of sensors. The synopsis is a bit vector of $\log(n)$ bits. Let $h()$ be a hash function from sensor-ids to $[1..\log(n)]$ such that a random $\frac{1}{2}$ of the domain maps to 1, $\frac{1}{4}$ maps to 2, $\frac{1}{8}$ maps to 3, etc. The SG function creates a bit vector of all 0's and then sets the $h(i)$'th bit to 1, where i is the sensor node's unique sensor-id. The SF function takes two bit vectors and outputs their bit-wise OR. The SE function takes a bit vector and outputs $2^{j-1}/0.77351$, where j is the index of the lowest-order unset bit. The approximation guarantees are provided in [7]—intuitively, if no node sets the jth bit then there are probably less than 2^j nodes. The algorithm avoids double-counting, intuitively, because each sensor i is associated with the $h(i)$'th bit being set and ORing that bit in multiple times is identical to ORing it in just once. The accuracy of this algorithm can be improved by using multiple bit vectors based on different hash functions, at a cost of sending longer messages [5, 17].

Other Related Work. Many papers have presented techniques for computing aggregates over data streams, including distributed data streams (see [2, 16] for surveys). Several recent papers [10, 23] have proposed duplicate-insensitive multi-path in-network aggregation techniques for peer-to-peer networks or mobile environments. None of their techniques are suitable for the sensor network setting in which reducing energy consumption is of paramount importance.

[1]For readers familiar with the synopsis diffusion framework, note that we will deviate slightly from [17] for some of the aggregates discussed in the paper (Frequent Items, Quantiles), by relaxing the requirement that the *same synopsis* be generated regardless of the aggregation topology.

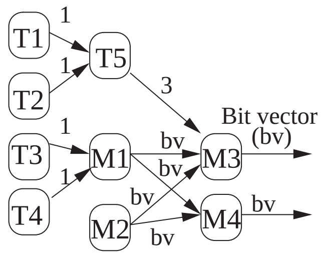

Figure 3: Combining Tree and Multi-path algorithms for computing Count in the Tributary-Delta framework.

In summary, none of the previous work has proposed and studied combining the complementary strengths of the two approaches in order to obtain the best of both (and more).

3. TRIBUTARY-DELTA APPROACH

In our Tributary-Delta aggregation scheme, we leverage the synergies between the existing energy-efficient schemes, by combining the efficiency and accuracy of (small) trees under low loss rates with the robustness of multi-path schemes. Specifically, part of the network runs a multi-path scheme while at the same time the rest of the network runs tree schemes. In the extreme, all nodes might either run a multi-path or a tree scheme. We dynamically adjust the use of trees and multi-path, based on current message loss rates. In this section we provide an overview of our Tributary-Delta scheme. We begin with the following observation.

Observation 1. *A Tributary-Delta aggregation process can be viewed as a directed graph G (representing the aggregation topology), where the sensors and the base station form the set of vertices, and there is a directed edge for each successful transmission. Each vertex is labeled either $\mathcal{M}$ (for multi-path) or $\mathcal{T}$ (for tree) depending on whether it runs a multi-path aggregation algorithm or a tree-based aggregation algorithm. An edge is assigned the same label as that of its source vertex. Note that both the set of edges and the labels of individual vertices and edges may change over time.*

Figure 1 depicts an example graph G, where the edges are directed to the right in the figure. Figure 3 depicts a portion of another example graph, where $T1$–$T5$ are $\mathcal{T}$ vertices and $M1$–$M4$ are $\mathcal{M}$ vertices.

There are many ways to construct an aggregation topology with both $\mathcal{M}$ and $\mathcal{T}$ vertices. The basic correctness criteria is that no two $\mathcal{M}$ vertices with partial results representing an overlapping set of sensors are connected to $\mathcal{T}$ vertices. This is necessary, since otherwise the corresponding $\mathcal{T}$ vertices, whose local aggregation algorithm is duplicate-sensitive, may double-count the same sensor data and provide incorrect answer. Formally, for every maximal subgraph G' consisting of $\mathcal{M}$ vertices, there is exactly one vertex $m \in G'$ directly connected to a $\mathcal{T}$ vertex in $G - G'$ and every vertex $v \in G'$ has a path to m. Ensuring this requires electing a suitable leader (m) within G'. This general construction, although achievable, thwarts our objectives: it restricts the amount of available redundancy an $\mathcal{M}$ vertex can exploit and the leader election process complicates the aggregation process.

We therefore restrict ourselves to a simpler model where a sensor receiving a partial result from an $\mathcal{M}$ vertex uses a multi-path aggregation scheme. This ensures that a partial result from an $\mathcal{M}$ vertex never reaches a $\mathcal{T}$ vertex downstream towards the base station, and therefore a $\mathcal{T}$ node never gets the chance to double-count sensor data. In terms of the graph, this correctness condition can be formulated as either an **Edge Correctness** property (Property 1) or a **Path Correctness** property (Property 2). The two properties are equivalent—both formulations are useful depending on the context.

PROPERTY 1. **Edge Correctness***: An $\mathcal{M}$ edge can never be incident on a $\mathcal{T}$ vertex, i.e., an $\mathcal{M}$ edge is always between two $\mathcal{M}$ vertices.*

PROPERTY 2. **Path Correctness***: In any directed path in G, a $\mathcal{T}$ edge can never appear after an $\mathcal{M}$ edge.*

An implication of *path correctness* is that the $\mathcal{M}$ vertices will form a subgraph (a multi-path "delta") that includes the base station, which is fed by trees of $\mathcal{T}$ vertices ("tributaries"), as depicted in Figure 1. Let the *delta region* of G be the set of $\mathcal{M}$ vertices. Coincidentally, graphs satisfying *path correctness* are also desirable for high accuracy—partial results near the base station account for larger numbers of sensor readings than partial results near the leaves of G, and hence the additional robustness provided by the delta region significantly improves the accuracy.

Our Tributary-Delta approach requires multi-path algorithms that can operate on (approximate or exact) partial results from both tree and multi-path schemes. For example, $M3$ in Figure 3 receives inputs from both a $\mathcal{T}$ vertex and two $\mathcal{M}$ vertices. We address this algorithmic challenge in Section 5.

Dynamic Adaptation. Our goal is to dynamically adapt where in the sensor network we use trees versus where we use multi-path, based on current message loss rates in various regions of the network. However, an implication of *edge correctness* is that individual vertices cannot switch between the two modes independently. We say an $\mathcal{M}$ vertex is *switchable* if all its incoming edges are $\mathcal{T}$ edges or it has no incoming edges. Similarly, a $\mathcal{T}$ vertex is *switchable* if its parent is an $\mathcal{M}$ vertex or it has no parent. In Figure 3, vertices $T3$, $T4$, $T5$, $M1$, and $M2$ are switchable. Based on these two definitions, we make the following observation.

OBSERVATION 2. **All** *children of a switchable $\mathcal{M}$ vertex are switchable $\mathcal{T}$ vertices.*

Note that a delta region uniquely defines the set of switchable $\mathcal{M}$ and $\mathcal{T}$ vertices in G. The next lemma implies that by considering only the *switchable* $\mathcal{T}$ and $\mathcal{M}$ vertices, it is always possible to expand (or shrink) the delta region if it makes sense to do so. Let G' be the connected component of G that includes the base station. Then expanding (shrinking) the delta region only makes sense if there is a $\mathcal{T}$ vertex (an $\mathcal{M}$ vertex, respectively) in G'. A simple induction proof yields the following result:

LEMMA 1. *If the set of $\mathcal{T}$ vertices in G' is not empty, at least one of them is switchable. If the set of $\mathcal{M}$ vertices in G' is not empty, at least one of them is switchable.*

In the next section, we study strategies for adjusting the tributaries and deltas for responding to changing network conditions and the synchronization issues arising due to dynamically switching between generating a $\mathcal{T}$ partial result and an $\mathcal{M}$ partial result. We defer to Section 5 the discussion of algorithmic challenges arising out of the dynamic network conditions.

4. ADAPTING TO NETWORK CONDITIONS

In this section we study in detail how our Tributary-Delta scheme dynamically adapts to changing network conditions.

4.1 Adaptation Design and Synchronization

Recall from Section 3 that the only possible ways to adapt to changing network conditions are to shrink the delta region by switching switchable multi-path ($\mathcal{M}$) nodes to tree ($\mathcal{T}$) nodes or to expand the delta region by switching switchable $\mathcal{T}$ nodes to $\mathcal{M}$ nodes. However, because of the different types of errors introduced by the tree and multi-path schemes (recall Table 1), it is unclear how switching one or more nodes impacts the answer accuracy. Therefore, we require users to specify a threshold on the minimum percentage of nodes that should contribute to the aggregate answer. It then becomes natural for the base station to be involved in the decision process: depending on the % of nodes contributing to the current result, the base station decides whether to shrink or expand the delta region for future results. Because there is only minimal communication error in multi-path schemes (recall Figure 2), increasing the delta region always increases the % contributing. Similarly, decreasing the delta region always decreases the % contributing. The system seeks to match the target % contributing, in order to take advantage of the smaller approximation error in tree aggregation. Because this design does not rely on the specifics of any one query, the resulting delta region is effective for a variety of concurrently running queries. Designs specialized to *particular* queries are part of our future work.

A key concern in switching individual nodes from tree aggregation to multi-path aggregation (and vice-versa) is how to ensure that nodes that should be communicating after the switch are indeed sending and receiving during the same epoch. When a node switches from $\mathcal{M}$ to $\mathcal{T}$, it needs to change its sending epoch to match its new parent's listening epoch and change its new children's sending epoch to match its listening epoch, etc. Conversely, when a node switches from $\mathcal{T}$ to $\mathcal{M}$, it needs to change its sending epoch to match the listening epoch of its neighboring nodes in the next level and change its children's sending epoch to match its listening epoch, etc. This re-synchronization overhead would arise, for example, if TAG [11], a popular tree aggregation approach, were used in conjunction with using rings for multi-path, and it could be a large deterrent to switching between tree and multi-path schemes. To ensure that no such re-synchronization is necessary, we make a simplifying design choice: a node in level i when switching from $\mathcal{M}$ to $\mathcal{T}$ must choose its parents from one of its neighbors in level $i-1$. Similarly, when the node switches from $\mathcal{T}$ to $\mathcal{M}$, it transmits to all its neighbors, including its parent, in level $i-1$. In other words, all tree links should be a subset of the links in the ring. This ensures that the switched node can retain its current epoch, since the new parent in level $(i-1)$ is already synchronized to receive data from the node in level i. Trees constructed with this restriction may have lessened link quality; however, this is mitigated with

Tributary-Delta because (1) we use multi-path to overcome poor link quality and (2) our tree construction algorithm (see Section 6.1.3), which guarantees that tree links are subsets of rings links, produces bushy trees that are effective in reducing total communication errors.

4.2 Adaptation Strategies

In this section, we present two alternative strategies to shrink and expand the delta region. In both strategies, we augment the messages being sent between sensor nodes with an (approximate) Count of the number of nodes that contributed to the partial result being sent. Assuming that the base station knows the total number of sensors in the network, it can compute the % of sensors that contributed to the current result.

Strategy `TD-Coarse`. In the first strategy, `TD-Coarse`, if the % contributing is below the user-specified threshold, the base station expands the delta region by broadcasting a message asking *all* the current switchable $\mathcal{T}$ nodes to switch to $\mathcal{M}$ nodes. This effectively widens the delta region by one level. Similarly, if the % contributing is well above the threshold, it shrinks the delta region by one level by switching *all* current switchable $\mathcal{M}$ nodes to $\mathcal{T}$ nodes. The coarse-grained control of `TD-Coarse` is well-suited to quickly adapting the size of the delta region to network-wide fluctuations. However, it can not adapt well to different conditions in different parts of the network; for this, we introduce the following more fine-grained strategy.

Strategy `TD`. In the second strategy, `TD`, we use the existence of the parent-child relationship among switchable $\mathcal{M}$ nodes and switchable $\mathcal{T}$ nodes (Observation 2), as follows. Each switchable $\mathcal{M}$ node includes in its outgoing messages an additional field that contains the number of nodes in its subtree that did *not* contribute.[2] As the multi-path aggregation is done, the maximum, *max*, and the minimum, *min*, of such numbers are maintained. If the % contributing is below the user-specified threshold, the base station expands the delta region by switching from $\mathcal{T}$ to $\mathcal{M}$ all children of switchable $\mathcal{M}$ nodes belonging to a subtree that has *max* nodes not contributing. In this way, subtrees with the greatest robustness problems are targeted for increased use of multi-path. Shrinking is done by switching each switchable $\mathcal{M}$ node whose subtree has only *min* nodes not contributing. The fine-grained control of `TD` facilitates adapting to non-uniform network conditions, at a cost of higher convergence time and additional message overhead because the base station needs to send one message every time it switches a small number of nodes. Note that there are many possible heuristics to improve the adaptivity of `TD`, such as using *max*/2 instead of *max* or maintaining the top-k values instead of just the top-1 value (*max*). We leave exploration of optimal heuristics for future work.

5. COMPUTING SIMPLE AGGREGATES

To compute an aggregate in our Tributary-Delta framework, we need a corresponding tree algorithm, a multi-path algorithm, and a *conversion function* that takes a partial result generated by the tree algorithm and outputs a synopsis that can be used by the multi-path algorithm. For example, in Figure 3, the node $M3$ receives two multi-path outputs (denoted as bv) and one tree output (3). The conversion function needs to transform the tree output to a synopsis so that $M3$ can use its synopsis fusion function to combine it.

The synopsis generated by the conversion function must be valid over the inputs from which the partial result has been generated by the tree algorithm. For example, the conversion function for the Count aggregate should take a partial aggregate C and generate a synopsis whose evaluation would produce the value C. This can be done by applying the Count synopsis generation function C times, or directly applying the Sum synopsis generation function [5] once. Intuitively, this enables a node running a multi-path algorithm to become oblivious to whether an input synopsis is generated by a node running the multi-path algorithm or by a node running the tree algorithm followed by applying the conversion function.

Many other aggregates (e.g., Sum, Min, Max, Average, Uniform sample, etc.) with known efficient multi-path [17] and tree algorithms have simple conversion functions (details omitted due to page limitations). Therefore, they can be efficiently computed in our Tributary-Delta framework. Moreover, the Uniform sample algorithm can be used to compute various other aggregates (e.g., Quantiles, Statistical moments) using the framework.

However, no efficient multi-path algorithm exists to compute an important aggregate: finding frequent items in the sensor network. This is an important aggregate, in particular in the context of biological and chemical sensors, where individual readings can be highly unreliable and it is necessary to get a consensus measure [21]. In the next section, we present an algorithm to do so, as well as an efficient tree algorithm and the corresponding conversion function. Together, these enable computing frequent items in our Tributary-Delta framework.

6. IDENTIFYING FREQUENT ITEMS

In this section we present the first energy-efficient Tributary-Delta algorithm for finding frequent items, describing first the tree scheme (Section 6.1), then the multi-path scheme (Section 6.2), and finally the conversion function (Section 6.3).

Following [15, 14], we consider the following formulation of the frequent items problem. Each of the m sensor nodes generates a collection of *items*. For example, an item can be a value of a sensor reading at a particular point in time. The same "item" may appear multiple times at one or more sensor nodes. Let $c(u)$ be the frequency of occurrence of item u over all m nodes. Given a user-supplied error tolerance ϵ, the goal is to obtain for each item u, an *ϵ-deficient count* $\tilde{c}(u)$ at the base station, where each $\tilde{c}(u)$ satisfies

$$\max\{0, c(u) - \epsilon \cdot N\} \leq \tilde{c}(u) \leq c(u)$$

and N denotes the sum of item occurrences across all items, i.e., $N = \sum_u c(u)$. By computing ϵ-deficient counts, communication is not wasted aggregating counts for rare items (i.e., items with $c(u) \leq \epsilon \cdot N$). Moreover, for small ϵ values, little error is introduced by using ϵ-deficient counting for frequent items (i.e., items with $c(u) \gg \epsilon N$). Given a user specified support threshold s ($s \gg \epsilon$), similar to [15, 14], we report as frequent all items with ϵ-deficient counts greater than $(s-\epsilon)N$, thus ensuring that there are no false negatives, and all false positives have frequency at least $(s - \epsilon)N$.

[2]Note that there is no double-counting here because it follows from the *path correctness* property that the node is the root of a unique subtree.

Algorithm 1: Generate a $\epsilon(k)$-summary (executed by all nodes, where k is the height of the node)

Input: summaries $\mathcal{S}_j = \langle n_j, \epsilon_j, \{(u, \tilde{c}_j(u))\}\rangle$ from each child j among the node's children $\mathcal{C}$, and its own summary $\mathcal{S}' = \langle n', 0, \{(u, \tilde{c}'(u))\}\rangle$
Output: single $\epsilon(k)$-summary $\mathcal{S} = \langle n, \epsilon(k), \{(u, \tilde{c}(u))\}\rangle$

```
1. Set $n := \sum_{j \in \mathcal{C}} n_j + n'$
2. For each $u \in \bigcup_{j \in \mathcal{C}} \mathcal{S}_j \cup \mathcal{S}'$, set $\tilde{c}(u) := \sum_{j \in \mathcal{C}} \tilde{c}_j(u) + \tilde{c}'(u)$
3. For each $u \in \mathcal{S}$, set $\tilde{c}(u) := \tilde{c}(u) - (\epsilon(k) \cdot n - \sum_{j \in \mathcal{C}} \epsilon_j \cdot n_j)$
   and if $\tilde{c}(u) \leq 0$ remove $(u, \tilde{c}(u))$ from $\mathcal{S}$
```

6.1 Tree Algorithm

In this subsection, we present our tree-based frequent items algorithm, MIN TOTAL-LOAD, the first algorithm for identifying frequent items that uses only $O(\frac{m}{\epsilon})$ words[3] of total communication, which is optimal. The algorithm's guarantees hold for a class of trees that arise naturally in sensor networks. Previous tree-based frequent items algorithms [8, 14, 21] provided only a weak bound of $O(\frac{m}{\epsilon} \log m)$ on total communication, even for the simplified case of balanced, regular trees.

6.1.1 Solution Approach and Challenges

A useful data structure encapsulating the partial result sent by a node X to its parent is a *summary*, defined as follows. A *summary* $\mathcal{S} = \langle N, \epsilon, \{(u, \tilde{c}(u))\}\rangle$ includes a (possibly empty) set of items u and their estimates $\tilde{c}(u)$. Each estimate $\tilde{c}(u)$ satisfies $\max\{0, c(u) - \epsilon \cdot N\} \leq \tilde{c}(u) \leq c(u)$, where $N = \sum_u c(u)$ such that $c(u)$ is the frequency of item u in the (multi-set) union of the multi-sets belonging to nodes in the subtree rooted at X. The salient property of a summary is that items with frequency at most $\epsilon \cdot N$ need not be stored, resulting in a smaller-sized summary and therefore, less communication.

Our approach (similar to [8, 14]) is to distribute the ϵ error tolerance among intermediate nodes in the tree. We make the error tolerance a function of the *height* of a node, which is defined recursively as follows: the height of a leaf node is 1; the height of any other node is one more than the maximum height of its children. Let $\epsilon(i)$ denote the error tolerance of a node with height i.

Algorithm 1 presents the steps to generate a summary for a node X of height k, for a generic setting of the $\epsilon(i)$'s. Proceeding level-by-level up the tree, each node uses Algorithm 1 to generate an $\epsilon(k)$-summary, until at last the base station outputs an $\epsilon(h)$-deficient count for each item, where h is the height of the base station. For correctness, we need $\epsilon(1) \leq \epsilon(2) \leq \ldots \leq \epsilon(h)$. As long as $\epsilon(h) \leq \epsilon$, the user-specified guarantee is met. The sequence $\epsilon(1), \ldots, \epsilon(h)$ is called the *precision gradient* [14], because the precision of the data gradually decreases as it traverses the aggregation tree.

Thus far the approach has been similar to [14]. The key new challenge we address is how to set a precision gradient that minimizes total communication and is not restricted to balanced, regular trees. We seek a precision gradient that minimizes worst case total communication over all possible input instances, and is not limited by how many items or what kind of items it can handle. Note that finding the right setting is challenging even for a regular tree. When minimizing the *maximum* load on a link, as considered in previous approaches [8, 14], it suffices to bound the load on each link. This is a *local* property: for a node of height k, Step 3 of Algorithm 1 implies that estimates for at most $\frac{1}{\epsilon(k)-\epsilon(k-1)}$ items will be present in the summary it sends on its outgoing link. Total communication, however, is a *global* property, and requires minimizing a sum. Indeed, it is not obvious how to set the precision gradient to achieve optimal worst case total communication.

[3]We adopt the standard convention that a *word* holds one item or one counter.

6.1.2 Solution: The MIN TOTAL-LOAD Algorithm

Since any node at height k has at least one child of height $k-1$, for any given tree, the number of nodes at height k can never be more than the number of nodes at height $k-1$. In particular, for a balanced, regular tree of degree d, the number of nodes at height k is $\frac{1}{d}$-th fraction of the corresponding number at height $k-1$. Moreover, from Step 3 of Algorithm 1, we know that the maximum number of counters a node at height k can send on its outgoing link is proportional to $\frac{1}{\epsilon(k)-\epsilon(k-1)}$. To minimize total communication, it is then necessary to have large $\epsilon(k) - \epsilon(k-1)$ for small k so that the total number of counters sent on the numerous such links outgoing from nodes of small height remain small. Care must be taken, however, to ensure that the product of $\frac{1}{\epsilon(k)-\epsilon(k-1)}$ and $\frac{1}{d^k}$ remains small even for large k. Our solution MIN TOTAL-LOAD balances the allocation by setting $\epsilon(1)$ to be a constant fraction of the final ϵ, and then making $\frac{1}{\epsilon(k)-\epsilon(k-1)}$ vary as c^k for some $c < d$ so that the total number of counters (product of $\frac{1}{\epsilon(k)-\epsilon(k-1)}$ and $\frac{1}{d^k}$) that could be possibly sent by all nodes at height k still decreases with increasing k. To extend our solution to non-regular trees, we exploit the observation that the maximum possible total communication of a tree (with our solution) can only decrease if nodes in an (initially balanced, regular) tree are replaced by nodes of lesser height.

Our solution is based on the notion of a d-dominating tree, which we define as follows. For any tree, let $H(i)$ denote the fraction of nodes having height at most i. Mathematically, $H(i) = \frac{1}{m}\sum_{j=1}^{i} h(j)$, where $h(j)$ denotes the number of nodes at height j and m denotes the total number of nodes.

d-dominating tree: For any $d \geq 1$, we say that a tree is *d-dominating* if for any $i \geq 1$, $H(i) \geq \frac{d-1}{d}(1 + \frac{1}{d} + \ldots + \frac{1}{d^{i-1}})$.

Note that for any tree, $h(i)$ is monotonically non-decreasing as i increases, so every tree is 1-dominating. From the definition of a d-dominating tree, it follows that a tree that is $(d+\delta)$-dominating is also d-dominating for any $\delta \geq 0$. Also, given any tree and a precision $\delta_1 > 0$, we can always find some d such that the tree is d-dominating, but not $(d+\delta_1)$-dominating. We refer to such a d as the *domination factor* for the tree.

Example 2. Consider a tree T_e with height 4 and the $h(i)$ values shown in Table 2. The table also shows the $h(i)$ and the $H(i)$ values of the two completely balanced, regular trees T_2 and T_3 of degree 2 and 3 respectively. As the table shows, $H(i)$ of $T_e \geq H(i)$ of T_2, for all i. Therefore, the example tree is 2-dominating. However, the tree is not 3-dominating, since $H(2)$ of $T_e < H(2)$ of T_3. Assuming the granularity of d is 0.05, it can be shown that T_e has a domination factor of 2, since T_2 is the highest degree tree that T_e can dominate (i.e., T_e is not 2.05 dominating).

	Example Tree T_e				Regular Tree T_2 $(d=2)$				Regular Tree T_3 $(d=3)$			
h	1	2	3	4	1	2	3	4	1	2	3	4
$h(i)$	37	10	6	1	8	4	2	1	27	9	3	1
$H(i)$	37/54	47/54	53/54	54/54	8/15	12/15	14/15	15/15	27/40	36/40	39/40	40/40

Table 2: Example of a 2-dominating tree.

We are now ready to present the precision gradient settings for our Min Total-load algorithm:

Lemma 2. *For any d-dominating tree of m nodes, where $d > 1$, a precision gradient setting of $\epsilon(i) = \epsilon \cdot (1-t)(1 + t + \ldots + t^{i-1})$ with $t = \frac{1}{\sqrt{d}}$ limits total communication to $(1 + \frac{2}{\sqrt{d}-1})\frac{m}{\epsilon}$.*

Proof. In Step 3 of Algorithm 1, the frequency estimate of each item u is decremented by at least $n \cdot (\epsilon(i) - \epsilon(i-1))$. Since $\sum_{u \in \mathcal{S}} \tilde{c}(u) \leq n$, frequency estimates for at most $\frac{1}{\epsilon(i)-\epsilon(i-1)} = \frac{d^{i/2}}{\epsilon \cdot (\sqrt{d}-1)}$ items are sent by a node at height i to its parent.

Furthermore, because the maximum number of possible estimates a node at height i can send on its outgoing link increases with its height ($\propto d^{i/2}$), the total communication for a d-dominating tree is bounded by a (hypothetical) tree in which exactly $\frac{d-1}{d}\frac{1}{d^{i-1}}$ fraction of the nodes occur at height i. Therefore, the total communication is bounded by:

$$\frac{m(d-1)}{d}\sum_{i=1}^{\infty}\frac{1}{(\epsilon(i)-\epsilon(i-1))d^{i-1}} = \frac{m(d-1)}{\epsilon\sqrt{d}(\sqrt{d}-1)}\sum_{i=1}^{\infty}\frac{1}{d^{(i-1)/2}}$$

$$\leq \frac{m}{\epsilon}\frac{d-1}{(\sqrt{d}-1)^2} = \frac{m}{\epsilon}\frac{\sqrt{d}+1}{\sqrt{d}-1} = \frac{m}{\epsilon}\left(1 + \frac{2}{\sqrt{d}-1}\right)$$

□

Observation 3. *As the constant factor $(1+\frac{2}{\sqrt{d}-1})$ shows, total communication decreases as d increases. Therefore, it is desirable to have aggregation trees which are d-dominating for large d values.*

A relatively straightforward induction proof yields the following result:

Lemma 3. *A tree in which each internal node of height i has at least d children of height $i-1$ is d-dominating.*

6.1.3 Trees with Large Domination Factors

As Lemma 2 shows, our Min Total-load algorithm works especially well for trees that are d-dominating for high d values. The chief concern for guaranteeing low communication is to ensure that the domination factor d is sufficiently far from 1, say at least 2. In Section 7, we show that a real-world sensor deployment has a domination factor of 2.25, suggesting that while it may be infeasible to construct a *regular* tree in a sensor network, it may be easy to generate d-dominating trees for $d \geq 2$. Moreover, we show next an explicit tree construction algorithm that seeks to increase the domination factor.

We modify the standard tree construction algorithm (described in Section 2) with two optimizations. First, when a node in level i chooses its parent, and even when it switches parents, it selects a node only from level $i-1$; the standard algorithm [11] allows choosing a parent from the same level. Second, we use the following *opportunistic parent switching* technique, inspired by Lemma 3. Each node of height $i+1$, if has two or more children of height i, pins down any two of its height i children, so that they cannot switch parents, and then flags itself. Next, the non-pinned nodes in each level j switch parents randomly to any other reachable non-flagged node in level $j-1$. As soon as a non-flagged node has at least two flagged children of the same height, it pins both of them and then flags itself. This local search technique quickly makes the tree 2-dominating if there is an opportunity to do so.

6.1.4 Extensions

Combining Objective Functions. Limiting total communication places an upper bound on the energy usage of all the sensors. However, in some cases, limiting the maximum load on a link is also very important [8, 14, 21]. We now show how to obtain a precision gradient setting that simultaneously achieves *both* optimal (within constant factors) maximum and optimal (within constant factors) total communication, by combining solutions that are optimal for each of the two individual metrics. Our combination technique can easily be generalized to multiple linear communication metrics, i.e., the communication metric is a weighted sum, weighted min, or weighted max of the communication load on the tree links. The following two observations are the key insights that lead to our technique.

Observation 4. *If each $\epsilon(i)$ in a precision gradient setting is divided by some constant $c \geq 1$, then the worst case value of any linear communication metric is multiplied by c.*

Observation 5. *For some $k \in [1,h]$, if the precision gradient setting is changed so that $\epsilon(i)$ is increased for $i \geq k$ and left unchanged otherwise, then the value of any linear communication metric does not increase.*

Lemma 4. *Let $\epsilon^a = (\epsilon(1)^a, \ldots, \epsilon(h)^a)$ and $\epsilon^b = (\epsilon(1)^b, \ldots, \epsilon(h)^b)$ denote the precision gradient settings that respectively minimize the* total communication *and the* maximum load on any link. *Then $\epsilon^* = (\epsilon(1)^*, \ldots, \epsilon(h)^*)$ where $\epsilon(i)^* = \frac{1}{2}(\epsilon(i)^a + \epsilon(i)^b)$ gives a simultaneous 2-approximation for* total communication *and* maximum load on any link.

Proof. Follows from Observation 4 and Observation 5. □

We call this variant of our algorithm Hybrid, because its objective function includes both maximum and total communication.

Computing Quantiles. The quantiles algorithm by Greenwald and Khanna [8] can be extended to use our precision gradients and hence to achieve useful bounds. For example, our techniques above for bounding total communication to $O(\frac{m}{\epsilon})$ words and for simultaneously bounding multiple communication metrics can be easily extended to the problem of *finding quantiles.* As such, they are the first quantiles algorithms that achieve these bounds. We formally state the technique analogous to Min Total-load for computing quantiles as Corollary 1.

Corollary 1. *If the quantiles algorithm provided by Greenwald and Khanna [8] is extended to use precision gradient, for any d-dominating tree of m nodes, where $d > 1$, a precision gradient setting of $\epsilon(i) = \epsilon \cdot (1-t)(1+t+\ldots+t^{i-1})$ with $t = \frac{1}{\sqrt{d}}$ permits the computation of quantiles with total communication at most $(1+\frac{2}{\sqrt{d}-1})\frac{m}{\epsilon}$.*

6.2 Multi-path Algorithm

We are aware of two previous multi-path algorithms for computing frequent items. The first algorithm, presented in [17], performs multi-path counting of the items in the network and keeps track of the items with high count values. Since the multi-path counting algorithm is approximate, it can find the frequent items only if they appear *significantly* more than the non-frequent items. The second algorithm computes a uniform sample of the items (which can be computed over multi-path as shown in [17]) and then estimates the frequent items over that sample. The accuracy of this algorithm depends on the sample size and the data distribution. As we show in Section 7, these two algorithms suffer from relatively high false positive and false negative rates under a real sensor dataset. We address this problem with a new multi-path algorithm for finding frequent items with high accuracy.

Ideally, we would like to base our algorithm on our tree algorithm (Algorithm 1), making it duplicate-insensitive so that it will work correctly in the multi-path setting. Steps 1 and 2 of Algorithm 1 are no problem: we simply replace the + operator in those steps with a known duplicate-insensitive addition operator. Step 3 is more problematic, however, because it uses a - operator and no duplicate-insensitive subtraction algorithms exist that combine high accuracy with small synopses.

Overcoming the Duplicate-Insensitive Subtraction Problem. Most duplicate-insensitive *addition* algorithms (for positive numbers) guarantee that the error in their estimates is at most a constant factor of the actual value. Specifically, for a user-specified relative error ϵ_c, $0 < \epsilon_c < 1$, and confidence parameter δ_c, $0 < \delta_c < 1$, the estimate is within a relative error ϵ_c of the actual sum with probability at least $1 - \delta_c$. Because each added item increases the actual sum, the allowed *absolute* error increases. If subtraction were allowed, the actual value would decrease and it is not known how to achieve a corresponding reduction in error while preserving a small synopsis.

Our solution is to avoid using subtraction altogether. First, we note that the primary purpose of the subtraction in Step 3 is to enable items with small estimated counts to be dropped from the summary. Instead of subtracting at each node and dropping the item if its estimate is negative, we eliminate the subtraction and drop the item if its estimate is below a rising threshold.

Second, we observe that we do not need highly accurate duplicate-insensitive addition in our thresholding approach. If we give ourselves some slack on the threshold, then we can tolerate less accurate addition and will not drop items we should not have dropped. We may fail to drop some items that should be dropped, but this does not change the asymptotic communication bounds. The importance of making use of less accurate addition arises from the fact that known duplicate-insensitive addition algorithms [3, 4, 5, 17] require synopses whose size is proportional to $\frac{1}{\epsilon_c^2}$. When $\epsilon_c = \frac{1}{2}$, this equals 4; when $\epsilon_c = \frac{1}{100}$, this equals 10,000.

Algorithm 2: Synopsis fusion function
Inputs: synopses $\mathcal{S}_1 = \langle \tilde{n}_1, \{(u, \tilde{c}_1(u))\}\rangle$ *and* $\mathcal{S}_2 = \langle \tilde{n}_2, \{(u, \tilde{c}_2(u))\}\rangle$*, of class* i
Output: synopsis $\mathcal{S} = \langle \tilde{n}, \{(u, \tilde{c}(u))\}\rangle$*, of either class* i *or* $i+1$

```
1. Set $\tilde{n} := \tilde{n}_1 \oplus \tilde{n}_2$
2. For each item $u \in (\mathcal{S}_1 \cup \mathcal{S}_2)$, add $(u, \tilde{c}_1(u) \oplus \tilde{c}_2(u))$ to $\mathcal{S}$
3. If $\tilde{n} > 2^{i+1}$, then increment the class of $\mathcal{S}$ from $i$ to $i+1$
   and for each item $u \in (\mathcal{S}_1 \cup \mathcal{S}_2)$:
   if $\frac{\epsilon \cdot \tilde{n}}{\log N} \geq \eta \cdot \tilde{c}(u)$, drop $(u, \tilde{c}(u))$ from $\mathcal{S}$ (We restrict $\eta > 1$)
```

Finally, our algorithm adapts from [8] the concept of *classes.* The idea is to have the error tolerance ϵ of a synopsis vary linearly with its class, the logarithm of the number of items it represents, and only combine synopses having the same class. Assuming there are no duplicates, doing so ensures that there is always an opportunity for further pruning once any two synopses are combined. Therefore, a synopsis never becomes too large. Even with duplicates, as our analysis later shows, the size of a synopsis does not grow beyond a constant factor of the case when there are no duplicates. Also, since the count for the total number of items represented by a synopsis is approximate, we assign the class of a synopsis as the logarithm of the synopsis's estimate of the total number of items it represents. As long as ϵ_c, the relative error parameter of $\oplus$ is less than 1, there are at most $\log N + 1$ classes of synopses varying from $i = 0, \ldots, \log N$.

We now describe the different components of our multi-path algorithm, using the terminology presented in Section 2.

Synopsis Generation. Each sensor node processes its collection of items by counting item frequencies and discarding (pruning) all items u whose frequency is less than or equal to $\frac{in'\epsilon}{\log N}$, where n' is the total number of items in its collection and $i = \lfloor \log n' \rfloor$. Then the node generates a class i synopsis by using a duplicate-insensitive addition algorithm to compute a frequency estimate of each remaining item. If the node is a leaf node, it forwards the synopsis to its parent.

Synopsis Fusion. Each intermediate node, in general, receives from each of its children at most a single synopsis of each class. After receiving all synopses from its children, beginning with the smallest class for which the node has a synopsis, the node starts combining two synopses of the same class using Algorithm 2 (the $\oplus$ operator denotes duplicate-insensitive addition), until it is left with at most one synopsis of each class. It then transmits the resulting collection of synopses to its parent. The parameter η controls the accepted slack in the thresholding procedure, as a function of the error parameter ϵ_c.

Synopsis Evaluation. Finally, at the base station, the frequency estimates corresponding to an item are simply added (again using $\oplus$) across all the different $\log N$ classes.

Accuracy and Communication Bounds. The accuracy and communication bounds of our algorithm are summarized in the following theorem. The bounds are in terms of the number of sensors m, the total number of items N, the user-specified error tolerance ϵ and confidence parameter δ, and the relative error parameter ϵ_c of $\oplus$, where ϵ, δ, and ϵ_c are each between 0 and 1. In addition, the bound assumes the following *accuracy preserving duplicate-insensitive sum* operator $\oplus$.

DEFINITION 1. *Suppose $X_{(\epsilon_c,\delta_c)}$ denotes an (ϵ_c, δ_c)-estimate of a scalar X, with a relative error of ϵ_c, and a confidence parameter of δ_c. Then, the operator $\oplus$ is called an accuracy preserving duplicate-insensitive sum operator if $X_{(\epsilon_c,\delta_c)} \oplus Y_{(\epsilon_c,\delta_c)} = Z_{(\epsilon_c,\delta_c)}$, where $Z = X + Y$.*

An example of accuracy preserving duplicate-insensitive sum operator can be found in [3].

THEOREM 1. *When $\oplus$ is a accuracy preserving duplicate-insensitive sum operator, then with probability at least $1-\delta$, for all item u, the algorithm produces estimated frequencies $\tilde{c}(u)$ such that $(1-\epsilon_c)(c(u)-\epsilon N) \leq \tilde{c}(u) \leq (1+\epsilon_c)c(u)$. Moreover, the maximum load on a link is $O(\frac{\log^2 N}{\epsilon} \cdot \frac{1}{\epsilon_c^2} \cdot \log(\frac{m \log N}{\epsilon\delta}))$ memory words.*

The proof is provided in Appendix A.

6.3 Tributary-Delta Algorithm

Recall from the discussion in Section 5 that to combine tree and multi-path algorithms, we need a conversion function that takes a partial result generated by the tree algorithm and outputs a synopsis that can be used by the multi-path algorithm. For frequent items, when using our tree and multi-path algorithms provided in Section 6.1 and Section 6.2 respectively, this conversion function can simply be the synopsis generation (SG) function of our multi-path algorithm, applied to the estimated frequencies of the tree algorithm. Specifically, we take the summary $\langle n, \epsilon(k), \{(u, \tilde{c}(u))\}\rangle$ from Algorithm 1 and view $\tilde{c}(u)$ as the actual frequency to which we apply the thresholding test of SG (Section 6.2), letting the n' in SG be the n from the summary, in order to create the synopsis. In this way, the final error in estimating the frequency of an item is at most the sum of the errors in the tree and the multi-path algorithm. So, given a user-specified error ϵ, we can obtain (approximate) ϵ-deficient counts in the Tributary-Delta framework, by running our tree-algorithm with error tolerance ϵ_a (where $\epsilon(k) \leq \epsilon_a$) and our multi-path algorithm with error tolerance ϵ_b, such that $\epsilon_a + \epsilon_b = \epsilon$.

7. EXPERIMENTAL RESULTS

In this section we evaluate our two proposed Tributary-Delta approaches, `TD-Coarse` and `TD`, in varying network conditions, using existing tree and multi-path approaches as baselines. We begin in Section 7.1 by describing the real-world data and the simulation environment we used. Then, in Section 7.2, we show the different ways in which `TD-Coarse` and `TD` adapt to changes in network conditions. Using a simple aggregate (Sum), we report the accuracy improvements of our proposed approaches over the baseline approaches in Section 7.3. Finally, in Section 7.4, we provide measurements of communication load for our frequent items algorithm MIN TOTAL-LOAD and evaluate `TD-Coarse` and `TD` for this more complex aggregate.

7.1 Methodology

We implement `TAG` [11], `SD` [17] and our proposed Tributary-Delta approaches, `TD-Coarse` and `TD`, within the TAG simulator [11]. `TAG` is a tree-based aggregation approach used by TinyDB [11], whereas `SD` (for Synopsis Diffusion) is a multi-path aggregation approach over Rings [17]. In each simulation run, we collect a single aggregate value every epoch for 100 epochs, unless noted otherwise. We begin data collection only after the underlying aggregation topologies become stable. Unless otherwise stated, we use Sum as the aggregate. In all the experiments, we use a variant of [7] (as in [5]) for achieving duplicate insensitive addition. We allow the Tributary-Delta approaches to adapt their topologies every 10 epochs. Recall from Section 4 that the adaptivity decisions in our proposed approaches are guided by a threshold on the percentage of nodes contributing to the aggregate. We use 90% as the threshold. We use 48-byte messages, as used by the TinyDB system. This allows us to fit 40 32-bit `Sum` synopses (with the help of run-length encoding [18]) within a single message, and produce an approximate Sum based on the average of these 40 estimates.

Scenarios. We use LABDATA, a scenario reconstructing a real deployment, and SYNTHETIC, a synthetic scenario with several failure models, for our experiments. Using actual sensor locations and knowledge of communication loss rates among sensors, LABDATA simulates a deployment of 54 sensors recording light conditions in the Intel Research Berkeley laboratory [9]. The dataset contains around 2.3 million sensor readings. The SYNTHETIC scenario is a deployment of 600 sensors placed randomly in a 20 *ft* $\times$ 20 *ft* grid, with a base station at location $(10, 10)$. We study two failure models for SYNTHETIC: GLOBAL(p), in which *all* nodes have a message loss rate of p, and REGIONAL(p_1, p_2), in which all nodes within the rectangular region $\{(0,0),(10,10)\}$ of the 20×20 deployment area experience a message loss rate of p_1 while other nodes have a message loss rate of p_2.

7.2 Adaptivity of `TD-Coarse` and `TD`

To demonstrate the different ways in which our two strategies adapt to changes in network conditions, we study the SYNTHETIC scenario under the two failure models. First, we apply the GLOBAL(p) failure model with increasing values of p. Figure 4(a) and Figure 4(b) show snapshots of the `TD-Coarse` approach when the loss rates are 0.2 and 0.3 respectively. As expected, the delta region expands as the loss rate p increases—depicted by an increase in the number of larger dots from Figure 4(a) to Figure 4(b). The snapshots for the `TD` approach are similar, except that the delta region increases gradually, instead of expanding by all switchable nodes at a time.

Second, we apply the REGIONAL(p_1, p_2) failure model with increasing p_1 and a fixed $p_2 = 0.05$. In `TD-Coarse`, because the delta region expands uniformly around the base station, all nodes near the base station are switched to multi-path, even those experiencing small message loss. In `TD`, this problem does not arise because the delta region expands only in the direction of the failure region. Figure 4(c) and Figure 4(d) capture pictorially the response of `TD` to such localized failures. Even at a high loss rate, in `TD`, the delta region mostly consists of nodes actually experiencing high loss rate.

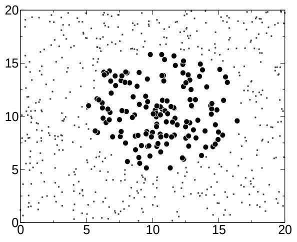
(a) TD-Coarse & Global(0.2)

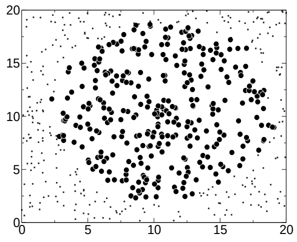
(b) TD-Coarse & Global(0.3)

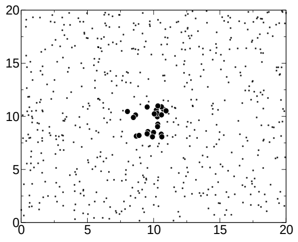
(c) TD & Regional(0.3,0.05)

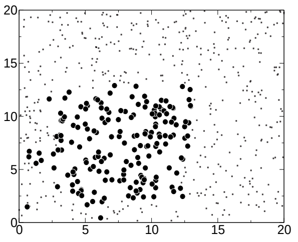
(d) TD & Regional(0.8,0.05)

Figure 4: Evolution of the TD-Coarse and TD topologies for varying loss rates. Each dot depicts a sensor located at the given coordinates in the deployment area. The larger dots comprise the delta region. The base station is at $(10, 10)$.

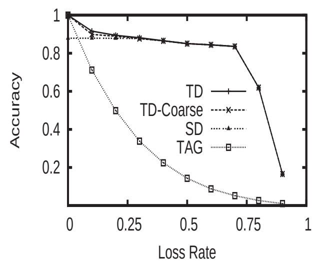

(a) Global failure

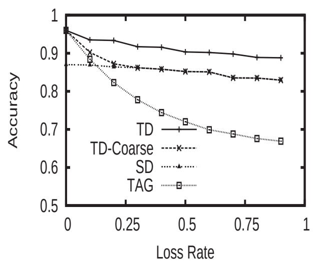

(b) Regional failure

Figure 5: RMS errors and loss rates.

7.3 Evaluation using a Simple Aggregate

In this section we evaluate the accuracy of our two proposed approaches in varying network conditions, using the TAG and SD approaches as baselines. We restrict ourselves to simple aggregates like Count and Sum for which the partial results can fit in a single TinyDB packet for both TAG and SD. To ensure that all approaches use comparable energy levels, we disallow retransmissions (as in the original TinyDB implementation).

For measuring *accuracy*, we use the relative root mean square (RMS) error—defined as $\frac{1}{V}\sqrt{\sum_{t=1}^{T}(V_t - V)^2/T}$, where V is the actual value and V_t is the aggregate computed at time t. The closer this value is to zero the closer the aggregate is to the actual value. We define *accuracy* to be 1 minus the RMS error.

Real scenario: LabData. We measure the accuracy of evaluating the Sum aggregate on LabData. We find the RMS error to be 0.5 for TAG and 0.12 for SD. Both TD and TD-Coarse can dynamically determine that running synopsis diffusion over most of the nodes gives a better accuracy and provides an RMS error of 0.1.

Synthetic scenarios. For the remainder of this section, we use Synthetic scenarios. Figure 5 presents the accuracy of the different schemes under varying failure scenarios, for the Count aggregate. In Figure 5(a) and Figure 5(b), we use the models Global(p) and Regional(p, 0.05), respectively, with varying p. (Figure 5(a) is the full graph corresponding to Figure 2 in Section 1.) At *all* loss rates in both cases, both TD-Coarse and TD are at least as accurate as TAG or SD. As Figure 5(a) shows, at loss rates ($0 \le p \le 0.05$) where the accuracy of TAG and SD are comparable, TD and TD-Coarse provide slightly better accuracy than either of the two approaches. This is a consequence of the delta region being small enough at those loss rates that some of the nodes generating tree aggregates can *directly* communicate with the base station, thereby avoiding the approximation errors of multi-path aggregation. The advantage of the TD scheme is more pronounced under the Regional failure model. Under regional failures, the accuracy of TD is strictly better than that of TAG because TD uses multi-path aggregation in the failure region. It is also better than TD-Coarse and SD because the delta region is extended in only one direction to encompass the failure region (akin to Figure 4(d)) and hence a significant portion of the tree nodes, with no communication loss, can directly talk to the base station without incurring the approximation error of multi-path aggregation.

Next, we evaluate our Tributary-Delta schemes under a dynamic scenario that uses the Global and Regional failure models at different instances of time. The goal is to demonstrate how well the schemes adapt with the underlying dynamics. We start with the Global(0) failure model. At time $t = 100$, we introduce the Regional(0.3, 0) failure model. Then at time $t = 200$, we switch to the Global(0.3) failure model. Finally, at time $t = 300$, we restore the failure model to be Global(0).

Figure 6 shows the relative errors of the answers provided by different schemes over time. We use relative error instead of RMS error because each data point corresponds to just a single aggregate answer. Figure 6(a) shows the performance of two existing approaches, TAG and SD. As expected, TAG provides better accuracy when the loss rate is small (i.e., for $t \in [0, 100]$ or $t \in [300, 400]$) while SD is more accurate when the loss rate is higher (i.e., for $t \in [100, 300]$).

Figure 6(b) and Figure 6(c) compare the relative errors of TD-Coarse and TD with the smallest of the errors given by TAG and SD. At a high level, both TD-Coarse and TD, when converged, have at most the error given by any of the two existing approaches. However, the graphs reveal a number of subtle differences between the two Tributary-Delta schemes. First, because TD can adjust its delta region in a finer granularity, it can converge to provide a more accurate result. Second, the coarse granularity of TD-Coarse has an adverse effect on its convergence. The delta region can continue expanding and shrinking around the optimal point (e.g., for $t \in [100, 150]$ in Figure 6(b)). The base station can use simple heuristics to stop the oscillation (e.g., at $t = 150$), but even then it may end up using a delta region larger than what is necessary. Finally, the benefits of TD comes at the cost of a convergence time higher than that of TD-Coarse. As shown in Figure 6(c), TD takes around 50 epochs to converge after the network condition changes. The time can be reduced by carefully choosing some parameters (e.g., how often the topology is adapted), a full exploration

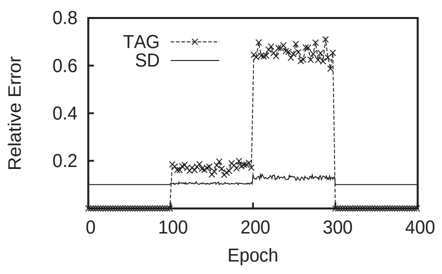

(a) TAG and SD

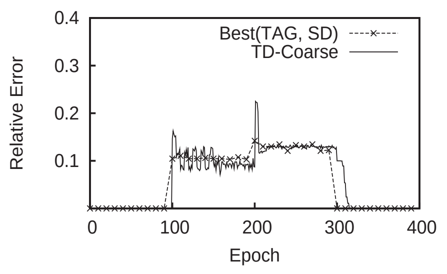

(b) TD-Coarse

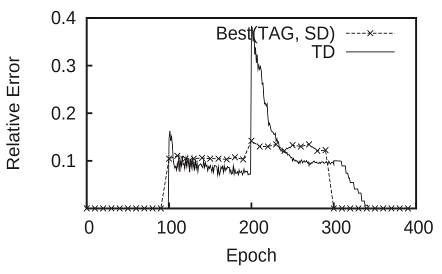

(c) TD

Figure 6: Timeline showing the relative errors of different aggregation schemes. (Note the changing y-axis scale.)

of which is beyond the scope of this paper.

7.4 Evaluation With Frequent Items

We begin in Section 7.4.1 by evaluating our tree construction algorithm presented in Section 6.1.3. Then, in Section 7.4.2, we evaluate MIN TOTAL-LOAD, our efficient frequent items algorithm for trees. In Section 7.4.3, we compare our multi-path algorithm with two related algorithms. Finally, in Section 7.4.4, we evaluate TD-Coarse and TD for the frequent items aggregate.

7.4.1 Evaluation of Tree Construction Algorithm

As mentioned in Section 6.1.3, our MIN TOTAL-LOAD algorithm has smaller overhead (by constant factors) if the aggregation tree is d-dominating for large d values. We note that, in practice, typical sensor deployments tend to have this property. For example, Figure 7(a) plots the cumulative number of nodes versus height for the aggregation tree of the LABDATA dataset. The distribution is lower bounded by the cumulative number of nodes of a balanced, regular tree with degree 2.25 (denoted as Regular(2.25)). Thus, that the aggregation tree of the LABDATA dataset is 2.25-dominating, which implies low overhead (the constant factor is 3 in this case).

Figure 7(b) and Figure 7(c) show the domination factors of the aggregation trees in different SYNTHETIC scenarios. In Figure 7(b), while keeping the deployment area fixed at 20×20, we vary the sensor density. In Figure 7(c), we keep the sensor density fixed (1 sensor per square unit area) and vary the size of the deployment area by changing its width (the height remains 20 across all experiments). The graphs show that our tree construction algorithm (Section 6.1.3) significantly improves the domination factor d. This is particularly useful when the domination factor of the tree is low because of low sensor density or narrow deployment area, since even a slight improvement in the d value greatly reduces the constant factor in MIN TOTAL-LOAD (which is proportional to $\frac{1}{\sqrt{d}-1}$).

7.4.2 Frequent Items over Tree

Figure 8 compares our two frequent items algorithms MIN TOTAL-LOAD (Section 6.1.2) and HYBRID, the 2-approximation algorithm presented in Section 6.1.4, against the two best known existing algorithms: MIN MAX-LOAD [14] and QUANTILES-BASED[4] [8]. We report the average and maximum load (number of integer values transmitted) of a node, under no message loss, on two sets of data. The first two sets

[4]Frequent items can be computed from quantiles.

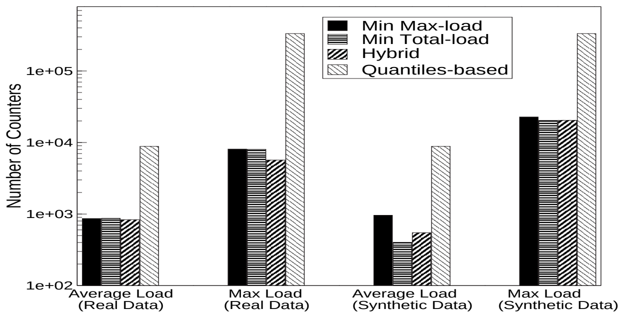

Figure 8: Average and maximum load of a sensor in a tree topology.

of bars in the graph represent the results with the LABDATA dataset. The graph shows that even though the communication load of our HYBRID algorithm is only guaranteed to be within a factor of 2 of the best of MIN TOTAL-LOAD and MIN MAX-LOAD, with our real world data set it performs significantly better. Specifically, HYBRID is 4% and 30% *better* than the best of MIN MAX-LOAD and MIN TOTAL-LOAD for average load and maximum load, respectively. It also shows that even though our MIN TOTAL-LOAD algorithm does not aim to reduce maximum load of a node, in practice it performs very close to MIN MAX-LOAD. The QUANTILES-BASED algorithm performs significantly worse than the other algorithms because it is not optimized for the bushy tree we encounter in LABDATA.

As discussed in Section 6.1, the average load for our MIN TOTAL-LOAD and HYBRID algorithms is upper bounded by a constant for any dataset (recall Lemma 2 and Lemma 4, noting that the average load is the total communication divided by the number of nodes), whereas it is logarithmic in the number of nodes for MIN MAX-LOAD and QUANTILES-BASED. Therefore, we can always construct a stream of items for which the improvement of MIN TOTAL-LOAD and HYBRID over MIN MAX-LOAD and QUANTILES-BASED is significant (e.g., zero vs. nonzero). As an example, in the last two sets of bars in Figure 8, we present results over a synthetic dataset, in which every sensor node receives a stream of items such that (1) the same item never occurs in multiple streams and (2) within a stream the items are uniformly distributed. As shown, MIN TOTAL-LOAD incurs only half the total communication required for the MIN MAX-LOAD algorithm (note the log-scale on the y-axis).

7.4.3 Frequent Items over multi-path

To understand the performance of our multi-path based

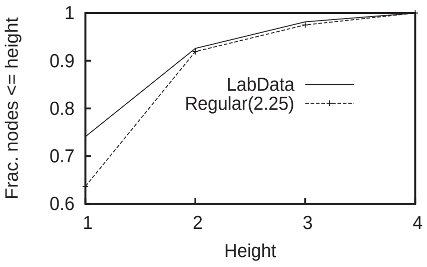

(a) LabData

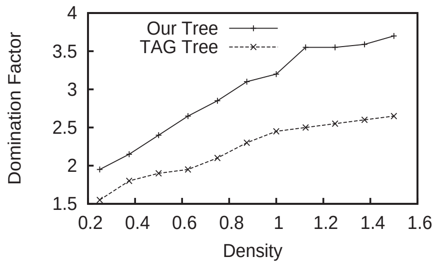

(b) Effect of density

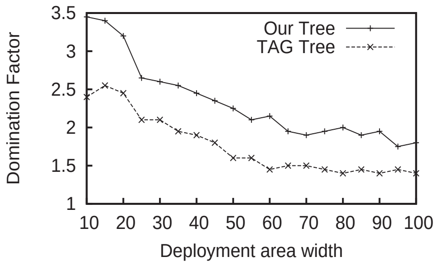

(c) Effect of deployment area shape

Figure 7: Domination factors in real and synthetic aggregation trees.

Algorithm	False positive	False negative
Min Total-load	2.3%	0
Counting-based	33.3%	30.3%
Sampling-based	15.4%	12.1%

Table 3: Average false positives and false negatives in the frequent items estimated by different multi-path algorithms.

Min Total-load algorithm, we compare it with the two existing algorithms mentioned in Section 6.2. We denote the first algorithm as Counting-based and the second algorithm as Sampling-based.

We use the Synthetic topology for this evaluation, with the brightness data stream of the LabData dataset evenly partitioned among the sensors. The real-valued sensor data are discretized with a bucket-size of 5 and Frequent Items are computed over these discrete values. In all cases, we aim to find all the items appearing more than 1% of the total number of item occurrences in the LabData. For a fair comparison, we use the sample size of Sampling-based and the synopsis size of Counting-based equal to the average message size (≈ 1000) of Min Total-load, so that they all have the same communication overhead. We measure the accuracy of the algorithms with their *false positive* (number of non-frequent items reported as frequent) and *false negative* (number of frequent items not reported) rates. Similar to the methodology in [14, 15], we use Min Total-load with error margin $\epsilon = 0.1\%$ to report all items with frequency more than the *support threshold* $s = 1\%$ of the total number of item occurrences in the LabData. However, because the count provided is ϵ-deficient, we actually report all the items whose estimated counts are more than $(s - \epsilon)$ of the total count. This introduces false positives in the result.

Table 3 shows the false positive and the false negative rates in the frequent items estimated by different algorithms. Each data point represents the average error over 100 experiments (each experiment has a random placement of sensors, and hence potentially a different topology). As shown, our Min Total-load algorithm has no false negative and has only a very small false positive rate. Counting-based suffers from large false positive and false negative rates since the distribution of the sensor data in LabData is not optimal for Counting-based—i.e., the frequent items do not appear significantly more than the non-frequent items. The false positive and the false negative rates of Sampling-based is higher than Min Total-load, implying that for this experiment, a sample size of 1000 is not sufficient for Sampling-based to achieve the accuracy provided by Min Total-load.

7.4.4 Frequent Items over Tributary-Delta

We now evaluate how well our Tributary-Delta algorithm finds frequent items. As mentioned in the previous section, Min Total-load has a small ($< 3\%$) false positive rate with no communication failure. Communication failures further reduces the false positive rate, but introduces false negatives in the estimated results. This is also because some of the items with frequency above the support threshold $s\%$ are not reported due to under estimation resulting from message loss.

Figure 9(a) and Figure 9(b) show the false negative rates of different aggregation schemes under the Global(p) and Regional($p, 0.05$) failure models, respectively. As in our previous results, `TD` performs as well as (for Global) or better than (for Regional) the `TAG` or `SD` schemes alone.

In contrast to the Sum or Count aggregate studied in Section 7.3, with the Frequent Items aggregate, a multi-path partial result can consist of more TinyDB messages (3 times on average in this experiment) than a tree partial result. Therefore, to make both approaches use comparable energy (i.e., a node transmits roughly the same number of bytes whether it is using a tree or a multi-path algorithm), we let the tree nodes retransmit their messages twice. The results are shown in Figure 9(c). As expected, retransmission significantly reduces the false negatives of the tree result. We argue that, even with retransmission, the `TD` approach is preferable. First, at a high loss rate (> 0.5 for Min Total-load), the multi-path algorithm still outperforms the tree algorithm and `TD` can effectively combine the benefits of both the algorithms. Second, epochs have to be longer to allow sufficient time for retransmissions, and hence the query latency increases linearly with the number of allowed retransmissions. The increased latency may be unacceptable to many real-time monitoring and control applications [22].

7.5 Summary of Results

Our results have quantified a number of advantages of our techniques. First, we have shown that our `TD-Coarse` and `TD` constructions can run tree and multi-path based aggregation simultaneously in different parts of the network and can dynamically balance between the tree and multi-path components as the operating conditions (e.g., loss rate) change. Second, Tributary-Delta is able to provide not just the best of the accuracies provided by tree or multi-path (e.g., by running either on them in the whole network), but in fact a significant accuracy improvement over the best, across a wide range of practical loss rates ($0 - 40\%$)—thus demonstrating

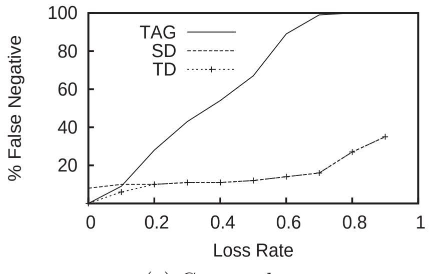

(a) Global loss

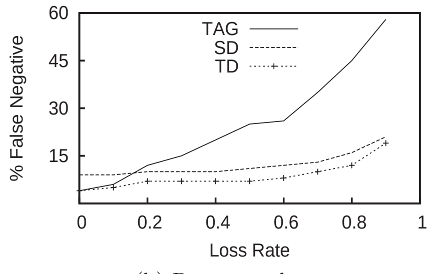

(b) Regional loss

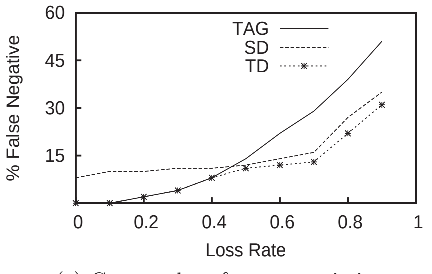

(c) Global loss & retransmission

Figure 9: False negatives in the estimated frequent items. (False positives are $< 3\%$)

the synergies of using both in tandem. For example, in computing Count under such loss rates, Tributary-Delta can reduce errors by up to a factor of 3 compared to an oracle that can dynamically choose the best existing approach (tree-based or multi-path-based) for a given loss rate. Moreover, Tributary-Delta never performs worse than such an oracle. Third, for complex queries (e.g., Frequent Items), Tributary-Delta may use larger messages than a tree-based algorithm do. However, Tributary-Delta can provide higher accuracy than a tree that retransmits messages on loss and hence consumes the same amount of communication energy.[5] For example, with our Frequent Items algorithm and within the loss rates $0 - 40\%$, Tributary-Delta reduces false-negatives by a factor of 4 compared to the best of `TAG` and `SD`. Thus, Tributary-Delta provides a sweet spot between communication overhead and approximation error, as shown in Table 1. Finally, we have shown that our tree-based and multi-path-based Frequent Items algorithms perform significantly better than the existing algorithms (Table 3).

8. CONCLUSIONS

In this paper, we have presented Tributary-Delta, a novel energy-efficient approach to in-network aggregation in sensor networks. Tributary-Delta combines the advantages of the existing tree- and multi-path-based approaches by running them simultaneously in different parts of the network. We have studied this new approach and presented schemes for adjusting the balance between tributaries and deltas in response to changes in network conditions. We have also shown how a difficult aggregate for this context—finding frequent items—can be efficiently computed in the Tributary-Delta framework. Our simulation results on real-world and synthetic data showed that our techniques are greatly superior to the existing tree- and multi-path-based approaches. For example, in computing Count under realistic loss rates, our techniques can reduce errors by up to a factor of 3 compared to *any* existing techniques.

9. REFERENCES

[1] Atmel AVR Microcontroller Datasheet. http://www.atmel.com/dyn/resources/prod_documents/2467s.pdf.

[2] B. Babcock, S. Babu, M. Datar, R. Motwani, and J. Widom. Models and issues in data stream systems. In *PODS*, 2002.

[3] Z. Bar-Yossef, T. Jayram, R. Kumar, D. Sivakumar, and L. Trevisan. Counting distinct elements in a data stream. In *RANDOM*, 2002.

[4] M. Bawa, A. Gionis, H. Garcia-Molina, and R. Motwani. The price of validity in dynamic networks. In *SIGMOD*, 2004.

[5] J. Considine, F. Li, G. Kollios, and J. Byers. Approximate aggregation techniques for sensor databases. In *ICDE*, 2004.

[6] A. Deshpande, C. Guestrin, S. Madden, J. M. Hellerstein, and W. Hong. Model-driven data acquisition in sensor networks. In *VLDB*, 2004.

[7] P. Flajolet and G. N. Martin. Probabilistic counting algorithms for database applications. *Journal of Computer and System Sciences*, 31:182–209, 1985.

[8] M. Greenwald and S. Khanna. Power-conserving computation of order-statistics over sensor networks. In *PODS*, 2004.

[9] Intel Lab Data. http://berkeley.intel-research.net/labdata/.

[10] D. Kempe, A. Dobra, and J. Gehrke. Gossip-based computation of aggregate information. In *FOCS*, 2003.

[11] S. Madden, M. J. Franklin, J. M. Hellerstein, and W. Hong. Tag: A tiny aggregation service for ad hoc sensor networks. In *OSDI*, 2002.

[12] S. Madden, M. J. Franklin, J. M. Hellerstein, and W. Hong. The design of an acquisational query processor for sensor networks. In *SIGMOD*, 2003.

[13] S. Madden, R. Szewczyk, M. J. Franklin, and D. Culler. Supporting aggregate queries over ad-hoc wireless sensor networks. In *WMCSA*, 2002.

[14] A. Manjhi, V. Shkapenyuk, K. Dhamdhere, and C. Olston. Finding (recently) frequent items in distributed data streams. In *ICDE*, 2005. To appear.

[15] G. Manku and R. Motwani. Approximate frequency counts over data streams. In *VLDB*, 2002.

[16] S. Muthukrishnan. Data streams: Algorithms and applications. Technical report, Rutgers University, Piscataway, NJ, 2003.

[17] S. Nath, P. B. Gibbons, S. Seshan, and Z. Anderson. Synopsis diffusion for robust aggregation in sensor networks. In *SenSys*, 2004.

[18] C. R. Palmer, P. B. Gibbons, and C. Faloutsos. ANF: A fast and scalable tool for data mining in massive graphs. In *SIGKDD*, 2002.

[19] B. Przydatek, D. Song, and A. Perrig. SIA: Secure information aggregation in sensor networks. In

[5]Note that a tree with retransmission also has a higher response time than a Tributary-Delta without retransmission.

SenSys, 2003.

[20] V. Shnayder, M. Hempstead, B.-R. Chen, G. W. Allen, and M. Welsh. Simulating the power consumption of large-scale sensor network applications. In *SenSys*, 2004.

[21] N. Shrivastava, C. Buragohain, D. Agrawal, and S. Suri. Medians and beyond: New aggregation techniques for sensor networks. In *SenSys*, 2004.

[22] G. Simon, A. Ledeczi, and M. Maroti. Sensor network-based countersniper system. In *SenSys*, 2004.

[23] Y. Tao, G. Kollios, J. Considine, F. Li, and D. Papadias. Spatio-temporal aggegeration using sketches. In *ICDE*, 2004.

[24] Y. Yao and J. Gehrke. Query processing in sensor networks. In *CIDR*, 2003.

[25] J. Zhao, R. Govindan, and D. Estrin. Computing aggregates for monitoring wireless sensor networks. In *SPNA*, 2003.

APPENDIX

A. PROOF OF THEOREM 1

Before stating and proving Theorem 1, we provide bounds on the accuracy of the synopsis generated at any node (Lemma 5), the accuracy of the synopses resulting from Synopsis Fusion (Lemma 6, Lemma 7 and Lemma 8), and bounds on the communication load on a link (Lemma 9, Lemma 10 and Lemma 11). Recall that all bounds are in terms of the number of sensors m, the total number of items N, the overall user-specified error tolerance ϵ and confidence parameter δ, and the relative error parameter ϵ_c of $\oplus$, where ϵ, δ, and ϵ_c are each between 0 and 1, and $\oplus$ is the constant error duplicate-insensitive sum operator defined in Definition 1.

We start with Lemma 5 which bounds the accuracy of the synopses generated by the nodes.

LEMMA 5. *With probability at least $1-\delta$, for any synopsis $\mathcal{S}$ generated at the nodes, and for any item u in $\mathcal{S}$, the following bounds hold:*

- $(1-\epsilon_c)\mathcal{S}.n \leq \mathcal{S}.\tilde{n} \leq (1+\epsilon_c)\mathcal{S}.n$
- $(1-\epsilon_c)\mathcal{S}.c(u) \leq \mathcal{S}.\tilde{c}(u) \leq (1+\epsilon_c)\mathcal{S}.c(u)$

PROOF. At each of the m sensor nodes, after the Synopsis Generation process, at most $\frac{\log \mathcal{S}.n}{\epsilon}$ locally frequent items remain. The union bound suggests that setting the confidence parameter for the duplicate-insensitive sum algorithm as $\delta_c = \frac{\epsilon\delta}{m \log N}$ is sufficient to have Lemma 5 hold. □

LEMMA 6. *With probability at least $1-\delta$, for any synopsis $\mathcal{S}$, $(1-\epsilon_c)\mathcal{S}.n \leq \mathcal{S}.\tilde{n} \leq (1+\epsilon_c)\mathcal{S}.n$. Moreover, if the class of $\mathcal{S}$ is i, $(1-\epsilon_c)2^i < \mathcal{S}.\tilde{n} \leq (1+\epsilon_c)2^{i+1}$.*

PROOF. Simple proof using induction. □

LEMMA 7. *With probability at least $1-\delta$, for any synopsis $\mathcal{S}$, the estimated frequency $\tilde{c}(u)$ of any item u satisfies: $\mathcal{S}.\tilde{c}(u) \leq (1+\epsilon_c)c(u)$.*

PROOF. By induction on $\mathcal{S}.\tilde{n}$.

Base step ($\mathcal{S}.\tilde{n}$): Such synopsis can only be generated by Synopsis Generation. If the item is not pruned, Lemma 5 applies. Or else, the lemma trivially holds.

Induction step: Either the synopsis is generated locally, or the synopsis is a result of invoking Synopsis Fusion. In case of the former, the *base step* argument applies. For the latter, Lemma 7 holds because $\oplus$ is constant error duplicate-insensitive sum and because of the induction assumption. □

LEMMA 8. *With probability $1-\delta$, for any synopsis $\mathcal{S}$ of class i, the estimated frequency $\tilde{c}(u)$ of any item u satisfies: $(1-\epsilon_c)(c(u) - \frac{i\epsilon\mathcal{S}.n}{\log N}) \leq \mathcal{S}.\tilde{c}(u)$*

PROOF. By Induction on $\mathcal{S}.\tilde{n}$.

Base step ($\mathcal{S}.\tilde{n}$ of class i): If u is pruned, $c(u) < \frac{i\epsilon\mathcal{S}.n}{\log N}$ and $\mathcal{S}.\tilde{c}(u) = 0$. Or else, Lemma 5 can be applied. In either case, Lemma 8 holds.

Induction step: If the synopsis is generated locally, the *base step* argument applies. Otherwise, it is a result of the synopsis fusion function. Let the two inputs to Synopsis Fusion be synopses $\mathcal{S}_1$ and $\mathcal{S}_2$ of class k. By induction assumption, $(1-\epsilon_c)(\mathcal{S}_1.c(u) - \frac{k\epsilon\mathcal{S}_1.n}{\log N}) \leq \mathcal{S}_1.\tilde{c}(u)$ and $(1-\epsilon_c)(\mathcal{S}_2.c(u) - \frac{k\epsilon\mathcal{S}_2.n}{\log N}) \leq \mathcal{S}_2.\tilde{c}(u)$. Let $\hat{c}(u)$ denote the frequency estimate of an item u before the pruning step. It follows that $(1-\epsilon_c)(\mathcal{S}_f.c(u) - \frac{k\epsilon\mathcal{S}_f.n}{\log N}) \leq \hat{c}(u)$. If item u is not pruned, $\mathcal{S}_f.\tilde{c}(u) = \hat{c}(u)$ and Lemma 8 holds (irrespective of whether the class of $\mathcal{S}$ increases or not). Or else, the class of S_f is $k+1$ and $\hat{c}(u) < \frac{\epsilon(1-\epsilon_c)\mathcal{S}.\tilde{n}}{(1+\epsilon_c)\log N}$. Using Lemma 5, $\hat{c}(u) < \frac{\epsilon(1-\epsilon_c)\mathcal{S}.n}{\log N}$. Hence, Lemma 8 holds. □

LEMMA 9. *For a synopsis $\mathcal{S}$ of class i, $\mathcal{S}.n < \frac{2^{i+1}}{1-\epsilon_c}$ with probability at least $(1-\delta)$.*

PROOF. Follows from Step (3) of Algorithm 2. □

LEMMA 10. *For any item u belonging to a class i synopsis $\mathcal{S}$, $\mathcal{S}.\tilde{c}(u) \geq \frac{(1-\epsilon_c)\epsilon 2^i}{(1+\epsilon_c)\log N}$ with probability at least $(1-\delta)$.*

PROOF. After synopsis generation, $\mathcal{S}.\tilde{c}(u) \geq \frac{i\epsilon 2^i}{\log N}$. In synopsis fusion, the class of a synopsis increases only in Step (3) and $\mathcal{S}.\tilde{c}(u) \geq \frac{(1-\epsilon_c)\epsilon 2^i}{(1+\epsilon_c)\log N}$ holds immediately after that. □

LEMMA 11. *The maximum number of (non-zero) frequency estimates in any class i synopsis $\mathcal{S}$ is $\frac{2(1+\epsilon_c)^2 \log N}{(1-\epsilon_c)^2 \epsilon}$.*

PROOF. Follows from Lemma 9 and Lemma 10. □

Proof of Theorem 1. Lemma 5, Lemma 7 and Lemma 8 provide accuracy bounds on the synopses generated by the synopsis fusion function. Since $\oplus$ is constant error duplicate-insensitive sum, the same bounds hold after synopsis evaluation too. The bound on communication load follows from Lemma 11.